Research Report

Effects of Energy Buffers in Distribution Grids with PV Generation

Carl Binding, Olle Sundström

IBM Research – Zurich
8803 Rüschlikon
Switzerland

IBM **Research**
   Almaden • Austin • Brazil • Cambridge • China • Haifa • India • Tokyo • Watson • Zurich

Effects of energy buffers in distribution grids with PV generation

Carl Binding and Olle Sundström

Abstract—The increased presence of photo-voltaic (PV) power generation in distribution grids has influences on the security of supply, in particular voltage stability. One of the commonly accepted control approaches to remediate over-voltage situations is the absorbing of reactive power by the PV inverters. An alternative approach is to introduce energy buffering devices (e.g. batteries) into the distribution grid and to control real power charged respectively discharged from the batteries. We have simulated an examplary rural distribution grid with PV generation and energy buffering in order to study the effect on voltage distribution and power flows.

I. INTRODUCTION

Solar power is present in most locations on the globe and, even in temperate climates, has a substantial peak intensity of approximately $1'000W/m^2$. Despite current PV technology's low efficiency - 20 % is a commonly quoted number [1] - the political will to increase the utilization of solar power for electrical energy generation is present in many geographies [2], [3]. It is accentuated by the CO_2 friendliness of the technology and as a potential, partial, substitute for nuclear power with its well known negative side-effects.

The impact of PV generation in distribution grids has been recognized [3] and potential remedies have been proposed. Berseneff [4] proposes the use of reactive power control in order to mitigate potential over-voltages in the distribution grid. Braun has studied the economical impact of using over-dimensioned PV inverters to generate sufficient amounts of reactive power for voltage control [5]. Work by Turitsyn et al. [6], [7] is also based on the PV inverter's capability to generate reactive power, illustrated in figure 1 and formalized in (1)

$$|Q_{max}(t)| = \sqrt{S_{max}^2 - P_{PV}(t)^2} \tag{1}$$

with Q_{max} the maximum obtainable reactive power, S_{max} the maximum apparent power of the PV inverter and $P_{PV}(t)$ the current real, solar power generated by a PV generator.

The principle of applying reactive power control to stabilize grid voltage is discussed in [8]. In a grid situation, one can formulate the voltage stability problem via control of reactive power Q as a non-linear, non-covex, optimal power-flow (OPF) optimization problem [4], [9] minimizing the overall line losses [1]. Various techniques have been proposed in the literature to solve the OPF [4], [10], [11]. Note however, that depending on the regulatory framework, PV generation - when
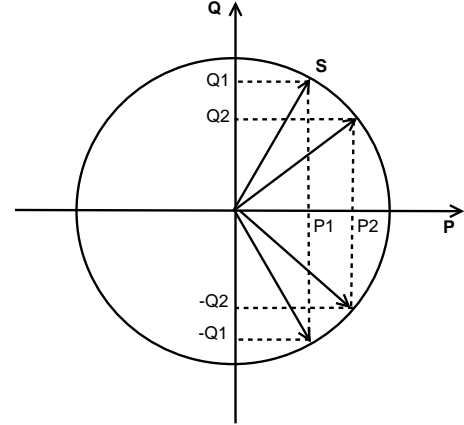
C. Binding and O. Sundström are with IBM Research–Zurich, 8803 Rüschlikon, Switzerland. (email: {cbd, osu}@zurich.ibm.com)

Figure 1. Maximal reactive power for photo-voltaic generators: For the real powers P_1 and P_2 we can obtain the indicated minimal, negative, and maximal, positive, reactive powers Q_1 and Q_2 given the maximal apparent power S.

below a given limit - must not necessarily provide any control features to the grid operator[1].

Turitsyn et al. [7] have linearized the optimization problem for reactive power control in a simple radial distribution grid, based on the *linear distribution flow* (LDF) [12]. It has the advantage of being computationally efficient and avoiding non-linear optimization constraints.

The target function to be minimized is of quadratic nature, namely

$$\sum_{i=0}^{n-1} r_i \frac{P_i^2 + Q_i^2}{V_0^2} \tag{2}$$

with n the number of nodes on the radial line, P_i, Q_i the real and reactive powers flowing on the line between node i and $i + 1$. V_0 is the voltage at node 0, i.e. the in-feed reference voltage, r_i the line resistance between nodes $i, i + 1$.

The constraints on the nodal power flows and voltages can then be expressed in a simplified linearized formulation using the approximation $V_i^2 \approx V_0^2 + 2V_0(V_i - V_0)$:

Real power flowing between nodes is given by:

$$P_{i+1} = P_i - p_{i+1}^{(c)} + p_{i+1}^{(g)}, \ i \in 0 \ldots n - 1 \tag{3}$$

with $p_i^{(c)}$ the consumed real power at node i and $p_i^{(g)}$ the generated real power at node i.

The formalization for reactive power flow is similar:

$$Q_{i+1} = Q_i - q_{i+1}^{(c)} + q_{i+1}^{(g)}, \ i \in 0 \ldots n - 1 \tag{4}$$

[1]In Germany, for example, a 100 kWp limit is given by [2].

with $q_i^{(c)}$ the consumed reactive power at node i and $q_i^{(g)}$ the generated reactive power at node i.

Finally, the voltage drop between nodes along the line is approximated to be:

$$V_{i+1} = V_i - (r_i P_i + x_i Q_i)/V_0, \ i \in 0 \ldots n-1 \quad (5)$$

with r_i and x_i the line resistance and reactance between nodes i and $i+1$.

In addition, the node voltages and variable reactive power values are constrained appropriately, equations (1) and (6).

$$V_0 - \epsilon \leq V_i \leq V_0 + \epsilon, i = 1 \ldots n \quad (6)$$

Whilst the control of reactive power is convenient and well suited to PV generation, the introduction of energy buffering devices (i.e. batteries) with the associated control of power charged respectively discharged has also been pursued [13], [14]. It has the following advantages over control through reactive power adjustment:

- *Voltage stability*: first and foremost, the objective remains to have nodal voltages within well defined limits, given by the appropriate grid-codes.
- *Balancing power generation peaks and valleys*: the presence of energy buffers allows for the local storage of excess energy and its release in times of insufficient solar power generation to satisfy local or non-local demand.
- *Micro-grid autonomy*: if the micro-grid were to be temporarily disconnected, the energy buffered might be sufficient to bridge periods of disconnectivity. However, the dimensioning of energy buffers will evidently increase substantially to handle such scenarios.

The literature reports various approaches to model and optimize the above scenario. Geidl and Andersson [15] propose an all-encompassing energy household model relying on electricity, natural gas, and district heat. PV generation is not specifically considered and the optimality criterion of the non-linear OPF is price of generation. Sortomme [16] uses particle swarm optimization (PSO) to solve the optimal power flow problem minimizing cost of generation. Constraints are formulated for voltage, real and reactive power, line-losses, controllable loads and battery power. Chandy et al. [17] study a single generator, single load (SGSL) system set-up using an OPF formulation on minimizing generation costs, battery usage cost and terminal costs. Voltage stability is of no concern, but the time-dimension of the problem is included: the battery energy level over time is constrained.

The remainder of the paper is organized as follows: Section II re-formulates the problem as a linearized OPF on a radial distribution grid. Our simulation set-up is discussed in section III. Results of the simulation are presented in section IV and we conclude the paper by a discussion and considerations of future work in section V.

II. PROBLEM FORMULATION

Our problem formulation is based on the work by Turitsyn et al., effectively using a linearized OPF. In addition to the constraints on the power flows and voltage levels (3)-(6), we have added the battery buffering constraints, i.e. limited power in- and out-flows as well as minimal and maximal energy levels over time.

The minimization target thus becomes

$$\sum_{t=0}^{T} \sum_{i=0}^{n-1} r_i \frac{P_i(t)^2 + Q_i(t)^2}{V_0(t)^2} + \sum_{t=0}^{T} P_{tot}(t) \quad (7)$$

where i denotes the iteration over the grid nodes and t iterates over a discretized time line ending a time-interval T. $P_{tot}(t)$ denotes the overall power balance of the micro-grid, including locally consumed power, locally generated (solar) power, power flowing in and out of the batteries, but neglecting line losses as formalized in (8).

$$P_{tot}(t) = \sum_{i=1}^{n} p_i^{(g)}(t) - p_i^{(c)}(t) - \sum_{j=1}^{n_{bat}} p_j^{(bat)}(t) \quad (8)$$

where j iterates over the number n_{bat} of batteries present in the system. Including the power total in the minimization target expresses the desire to minimize in-flows of power from the grid into the micro-grid, making the micro-grid as autonomous as possible.

The energy constraints on the batteries are formulated as follows:

$$e_{min_j}^{(bat)} \leq e_{0_j}^{(bat)} + \sum_{t=0}^{T} p_j^{(bat)}(t)\Delta t \leq e_{max_j}^{(bat)} \quad (9)$$

i.e. the power flows in and out of batteries integrated over the time-intervals must not exceed pre-defined limits. $e_{0_j}^{(bat)}$ is the initial energy contained in the battery at $t = 0$, $e_{min_j}^{(bat)}$ respectively $e_{max_j}^{(bat)}$ denote the minimal and maximal energy levels of the battery j, and Δt is the duration of a time-interval used in the discretization of time.

III. SIMULATION SET-UP

Our simulation uses well-known load profiles for domestic, farming, or services based loads [18]. Solar generation is simulated based on real solar data, recorded with a sampling interval of 10 minutes[2].

The simulation uses the grid shown in figure 2. Two nodes (11, 19) have solar panels with peak-powers of 240 kWp and 288 kWp respectively with a fixed $cos(\phi) = 0.95$ (inductive)[3]. We have used typical distribution cable data, using $R' = 0.206$ ohm/km and $L' = 0.08$ ohm/km [19]. The distances between nodes represent typical sub-urban distribution grids, nodes (5, 12, 15, 16) have two households attached to it. The influences of the drop-lines to individual households were neglected.

Batteries are placed at the grid nodes with solar panels. Their power rating is set to 200 kW; the energy capacities are

---

[2]Which is too high since solar power can largely fluctuate more rapidly, but useful for initial experimentation.

[3]These are large, but not unrealistic PV panel sizes depending on latitude and altitude.
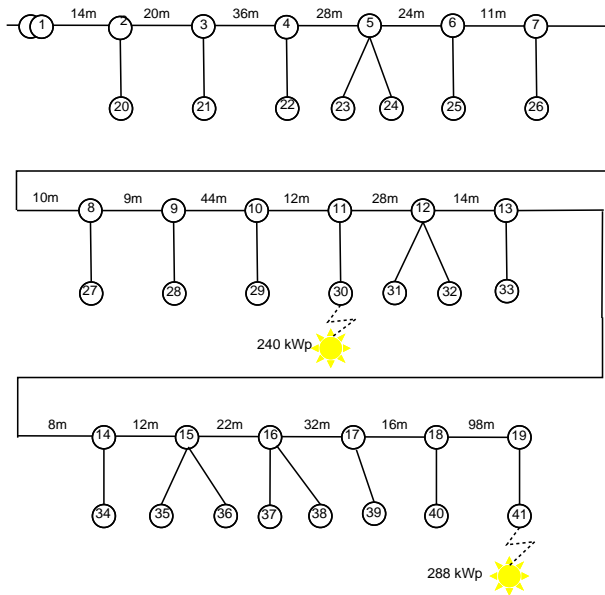
Figure 2. Sample distribution grid: nodes are numbered 1 to 41, distances between drop-offs are in meters. Solar generation occurs at nodes 30 and 41 with the indicated peak power.
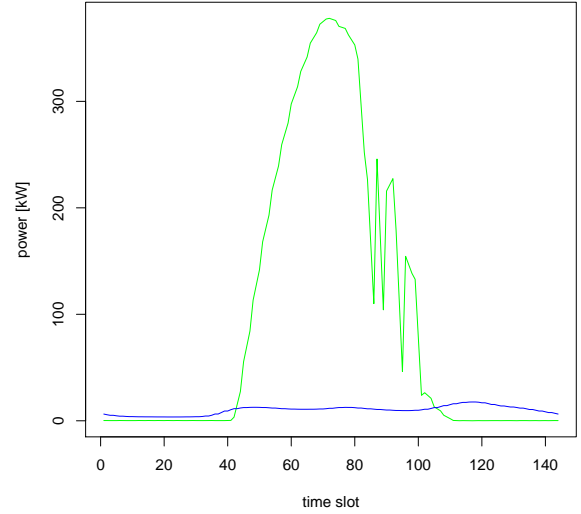

Figure 3. Consumed and solar-generated power: generated solar power far exceeds load consumption.

initially set to 720 kWh (node 11) and 864 kWh (node 19) respectively[4].

The simulation is run in two set-ups:

- time horizon of 24 hours: we use a full day (i.e. 144 slots of 10 minutes) to balance out the power-flow in and out of the batteries in order to minimize the inflowing power and keeping the nodal voltages within limits.
- time horizon of 2 hours: the optimization horizon is two hours during which battery power is used to stabilize the micro-grid voltages; each two hour period is independent of previous periods.

In both cases, we start out with empty batteries.

After balancing the grid in order to satisfy the linearized optimization problem of section II, we run a complete load flow using the obtain battery power settings. The resulting node voltages are then tested on under- and over-voltage conditions.

The power balances are shown in figure 3. Given the sizing of the solar panels, we have considerable excess in generating capabilities compared to the local demand. We also observe the solar generation peaking around mid-day with some brief interruptions in the early afternoon. The typical consumption peaks in the morning, noon, and evening are present but relatively small when compared with the amount of peak solar power generated.

IV. SIMULATION RESULTS

Figure 4 illustrates the over-voltages occurring towards the end of the distribution lines, between nodes 10 to 19. During

[4]Which is related to the peak power of the associated solar panel and some average daily sun-shine duration.

the midday time-slots, solar generation is peaking and thus we observe over-voltages of up to 1.12 p.u.
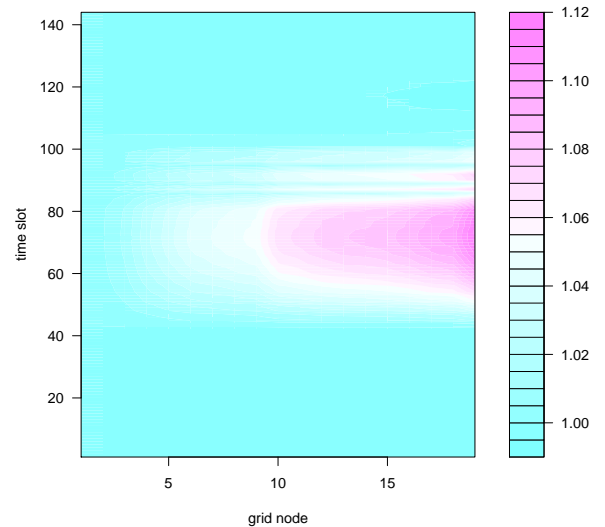

Figure 4. Over-voltages on radial distribution line

The 24 hour time-horizon optimization is shown in figure 5. Small increases in the nodal voltages occur around midday, as expected in periods of intensive solar power generation.

Figure 6 shows the 2 hour planning cycle. Note that, like for the case of 24 hours planning, there are no over-voltages. However, there are somewhat more frequent slight over-voltages in the time-slots 60-100.

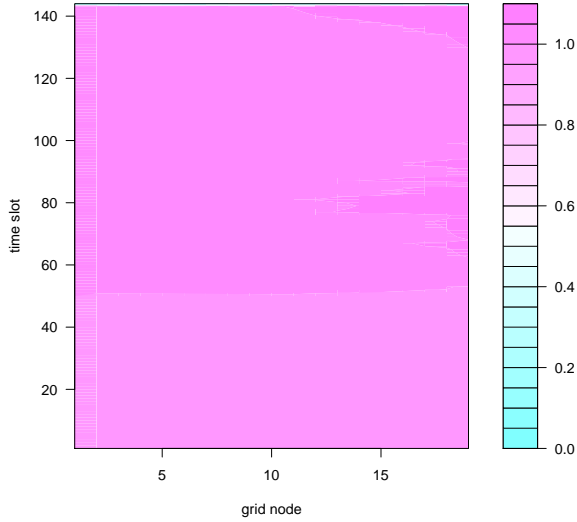Observing the state of energy in the (idealized) batteries, we

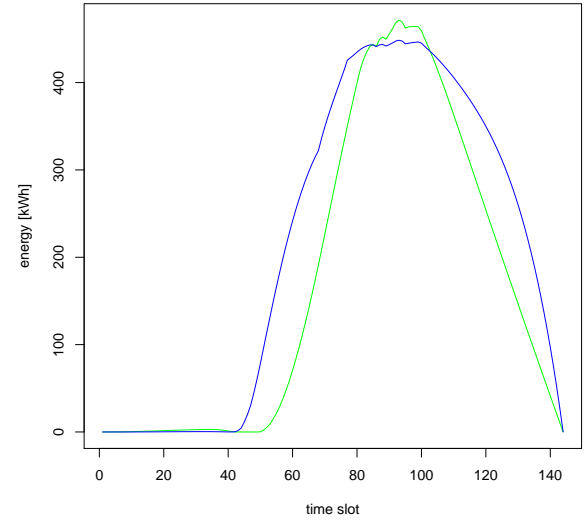Figure 5. Balanced node voltages, 24 hour time-horizon

Figure 7. Energy levels, 24 hour time-horizon: the dark line is the energy balance for the battery located at node 30, the lighter line relates to the battery at node 41.
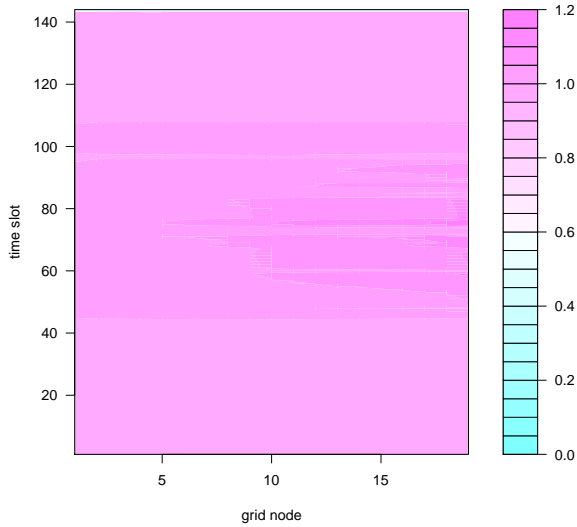

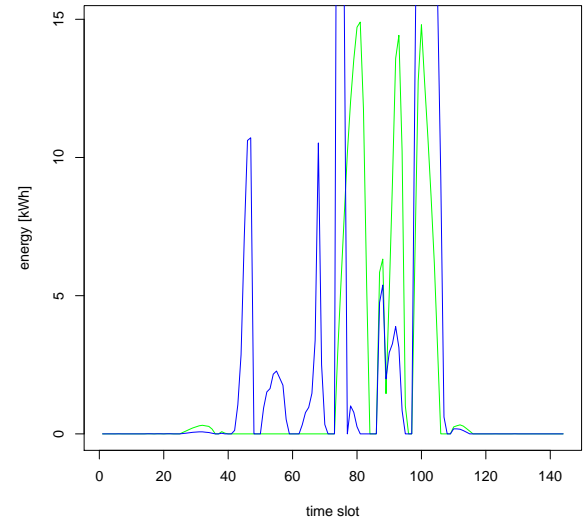
Figure 6. Balanced node voltages, 2 hour time-horizon

Figure 8. Energy levels, 2 hour time-horizon: the dark line is the energy balance for the battery located at node 30, the lighter line relates to the battery at node 41.

obtain the plots of figure 7 and 8. The vertical axes indicates the stored energy in the batteries, in [kWh]; the horizontal axis represents the time-slots. As expected, we observe the battery to be filled at a higher level during the peak sun-shine hours around midday. Although the overall capacities of the batteries are within the same order of magnitude, the battery towards the end of the distribution line is absorbing less excessive power and thus exhibits lower energy volumes. Overall we note that the batteries are not charged to their maximum of 720 kWh and 864 kWh respectively.

One can also observe a substantial difference in the behaviours of the 2 vs. 24 hours planning cycle. Using a shorter planning period, energy is fed-back into the grid more frequently when compared with the 24 hour planning - even when solar generation exceeds local (fixed) demand. This can be explained intuitively as follows: in the 2 hour planning period, the time-horizon beyond the plan duration is not seen and, since the overall grid power is part of the minimization objective, the battery is discharged without consideration of future use. This behaviour is also apparent in the 24 hour plan duration: the discharge also occurs towards the end of the plan.

Reducing the battery energy volumes to 40 kWh each, we obtain figure 9 for the 24 hour planning cycle. Not suprisingly, one of the batteries reaches its maximum energy level, whereas the other battery stays well below its maximum. The fluctuations around the maximally reached levels occur in
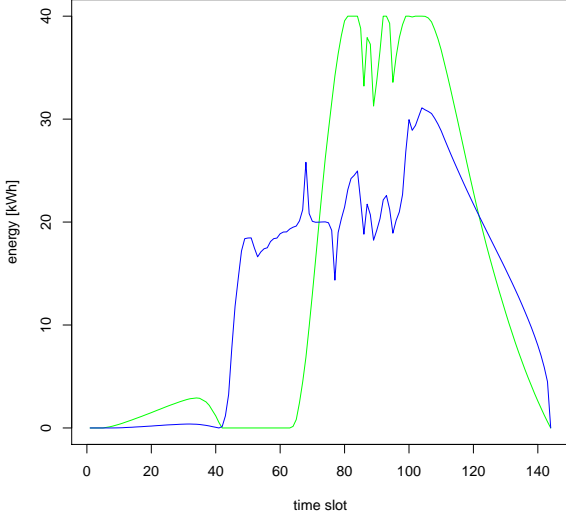

Figure 9. Energy levels, 24 hour time-horizon, reduced battery capacity: the dark line is the energy balance for the battery located at node 30, the lighter line relates to the battery at node 41.

time-slots 80 to 100 when solar generation also varies.

The total power in-, respectively out-flow of the micro-grid of figure 2 is represented in figure 10[5]. We show a curve for the small battery sizes (40 kWh each) and the larger battery sizes (720 and 864 kWh). As expected, there is feedback during times of abundant solar generation in both cases. For the larger batteries, the in-feed into the grid is less extreme (darker line) during peak solar generation, but it extends well into the evening hours when solar generation has ceased and the buffers are fed back into the overall grid. Note that the depletion of battery energy towards the end of the planning period could be controlled by tightening the constraints on energy levels or constraining the power flow from the micro-grid into the grid ($P_{tot}(t)$). The settings of operational limits would be up to the operator (DSO).

Figure 11 illustrates the influence of the sizing of the solar panels onto the over-voltages, without the influence of any batteries. Surprisingly the relationship between over-voltages and solar panel size is almost linear and, as expected, increases with the size of the panels.

When analyzing the influence on the battery size versus the PV panel sizes, we notice no influence on the battery size onto over-voltages. In figure 12 the increase in voltage can be seen - it however remains below 1.1 p.u. due to the use of the

---

[5]Negative values indicate power flow from the micro-grid into the larger grid.
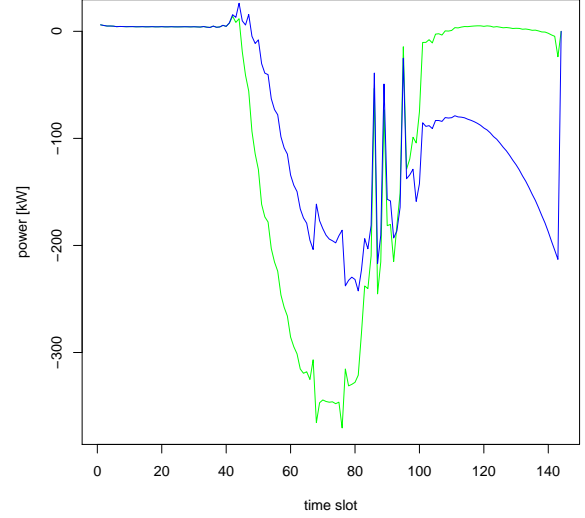

Figure 10. Power balances of micro-grid: the dark line shows the behaviour for the larger batteries, the lighter line is the power feedback when using two batteries of 40 kWh each.
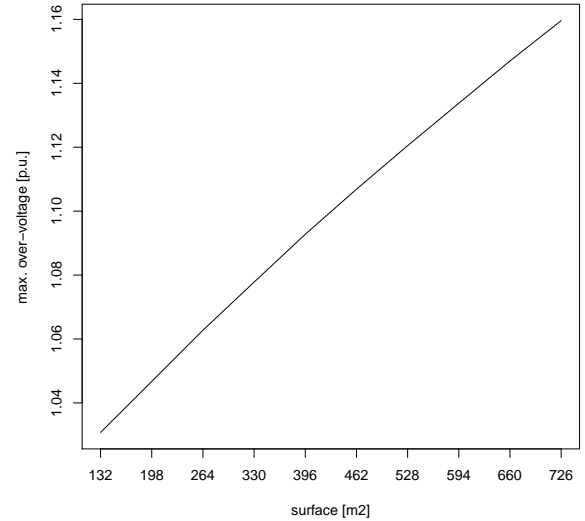

Figure 11. Over-voltages as function of PV panel size: sizes range from 132..720 [m^2].

batteries. Unlike the PV panel size, the battery sizes have no influence on the maximum voltage levels.

V. DISCUSSION

We have illustrated the effects of introducing local storage capabilities in a micro-grid with high level of photo-voltaic, decentralized, power generation. Instead of using the conventional control of reactive power, we control the real power flow by using local batteries to avoid over-voltages. Our simulation validates the approach, which – in addition to voltage stability
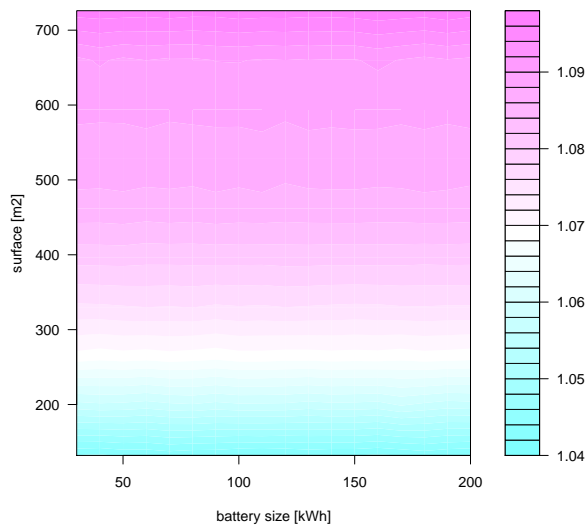
Figure 12. Over-voltages as function of PV panel sizes (132..720 $[m^2]$) and battery sizings (in [kWh])

– leads to a smoother overall power balance between the distribution grid and feeder lines as well as potential autonomy in cases of grid disconnection.

A largely dimensioned solar generation set-up was chosen as well as large and powerful batteries, in order to illustrate qualitative behaviour.

Investment and operational costs of the necessary batteries were not considered in our work. Battery placement has been chosen co-located with the decentralized generation; effects of other choices of location have not been considered. An optimization of battery placement, their numbers, and their sizing can be studied further.

We currently use a linearized OPF formulation to simulate the micro-grid which we revalidate with a load-flow computation. Non-linearized OPF can be used for a higher precision solution which also can handle more complex microgrid topologies. The linearized OPF can however be extended recursively for tree-shaped, radial distribution grids which are common in practice and which leads to good computational performance which is necessary considering the high variability of PV generation.

REFERENCES

[1] V. Crastan, *Elektrische Energieversorgung II*. Springer Verlag, 2004.
[2] Bundesregierung Deutschland, "Erneuerbare-Energien-Gesetz (eeg)," January 2009.
[3] E. Liu and J. Bebic, "Distribution system voltage performance analysis for high-penetration photovoltaics," National Renewable Energy Laboratory (NREL), Tech. Rep. NREL/SR-581-42298, February 2008.
[4] B. Berseneff, "Réglage de la tension dans les réseaux de distribution du futur," Ph.D. dissertation, Institut polytechnique de Grenoble, 2010.
[5] M. Braun, "Reactive Power Supplied by PV Inverters: Cost-Benefit-Analysis," in *22nd European Photovoltaic Solar Energy Conference and Exhibition*, Milano, Italy, September 2007.
[6] K. Turitsyn, P. Šulc, S. Backhaus, and M. Chertkov, "Distributed control of reactive power flow in a radial distribution circuit with high photovoltaic penetration," in *Proceedingds Power and Energy Society General Meeting (PES)*. Minneapolis, MN: IEEE, July 2010, pp. 1–6.
[7] ——, "Local control of reactive power by distributed photovoltaic generators," in *Proceedingds IEEE Int. Conference on Smart Grid Communications (SmartGridComm 2010)*. Gaithersburg, MD: IEEE, October 2010, pp. 79–84.
[8] P. Kundur, *Power System Stability and Control*. McGraw-Hill, 1994.
[9] F. Capitanescu, M. Glavic, D. Ernst, and L. Wehenkel, "Interior-point based algorithms for the solution of optimal power flow problem," *Electric Power Research*, vol. 77, pp. 508–517, 2007.
[10] N. Grudinin, "Reactive power optimization using successive quadtratic programming method," *IEEE Transactions on Power Systems*, vol. 13, no. 4, pp. 1219–1225, November 1998.
[11] J. Zhu, *Optimization of Powr System Operation*, ser. IEEE Press Series on Power Engineering. Wiley and Sons, 2009.
[12] M. E. Baran and F. F. Wu, "Optimal sizing of capacitors placed on a radial distribution system," *IEEE Transactions on Power Delivery*, vol. 4, no. 1, pp. 735–743, January 1989.
[13] X. Vallvé, A. Graillot, S. Gual, and H. Colin, "Micro storage and demand side management in distributed pv grid-connected installations," in *Porceedings of 9th International Conference on Electrical Power Quality and Utilization*, Barcelona, Spain, October 2007.
[14] T. Tanabae, Y. Udea, S. Suzuki, N. Sasaki, T. Tanaka, T. Funabashi, and R. Yokoyama, "Optimized operation and stabilization of microgrids with multiple energy resources," in *Proceedings of the 7th International Conference on Power Electronics*, Daegu, Korea, October 2007.
[15] M. Geidl and G. Andersson, "A modeling and optimization approach for multiple energy carrier power flow," in *Proceedings of IEEE PES PowerTech*, St. Petersburg, Russia, June 2005.
[16] E. Sortomme and M. A. El-Sharkawi, "Optimal power flow for a system of microgrids with controllable loads and battery storage," in *Proceedings of Power System Conference and Exposition*, Seattle, WA, March 2009.
[17] K. M. Chandy, S. Low, U. Topcu, and H. Xu, "A simple optimal power flow model with energy storage," in *49th IEEE Conference on Decision and Control*, Atlanta, GA, December 2010, pp. 15–17.
[18] R. Tiedemann and C. Fünfgeld, *Die Repräsentativen VDEW-Lastprofile - Der Fahrplan, Version 3.7*, VWEW Energieverlag, Frankfurt/Main, Germany, 2006.
[19] *Nexans: Niederspannungskabel*, Nexans Schweiz AG, Cortaillod, Switzerland, http://www.nexans.ch.